Ge $4s^2$ Lone Pairs and Band Alignments in GeS and GeSe for Photovoltaics - Supplementary Information

Matthew J. Smiles,[†] Jonathan M. Skelton,[*,‡] Huw Shiel,[†] Leanne A. H. Jones,[†] Jack E. N. Swallow,[¶] Holly J. Edwards,[†] Philip A. E. Murgatroyd,[†] Thomas J. Featherstone,[†] Pardeep K. Thakur,[§] Tien-Lin Lee,[§] Vin R. Dhanak,[†] and Tim D. Veal[*,†]

†*Stephenson Institute for Renewable Energy and Department of Physics, University of Liverpool, Liverpool, L69 7ZF, UK*

‡*Department of Chemistry, University of Manchester, Oxford Road, Manchester, M13 9PL, UK*

¶*Department of Materials, University of Oxford, Parks Road, Oxford, OX1 3PH, UK*

§*Diamond Light Source Ltd., Harwell Science and Innovation Campus, Didcot, Oxfordshire OX11 0DE, UK*

E-mail: jonathan.skelton@manchester.ac.uk; T.Veal@liverpool.ac.uk

Valence band spectra

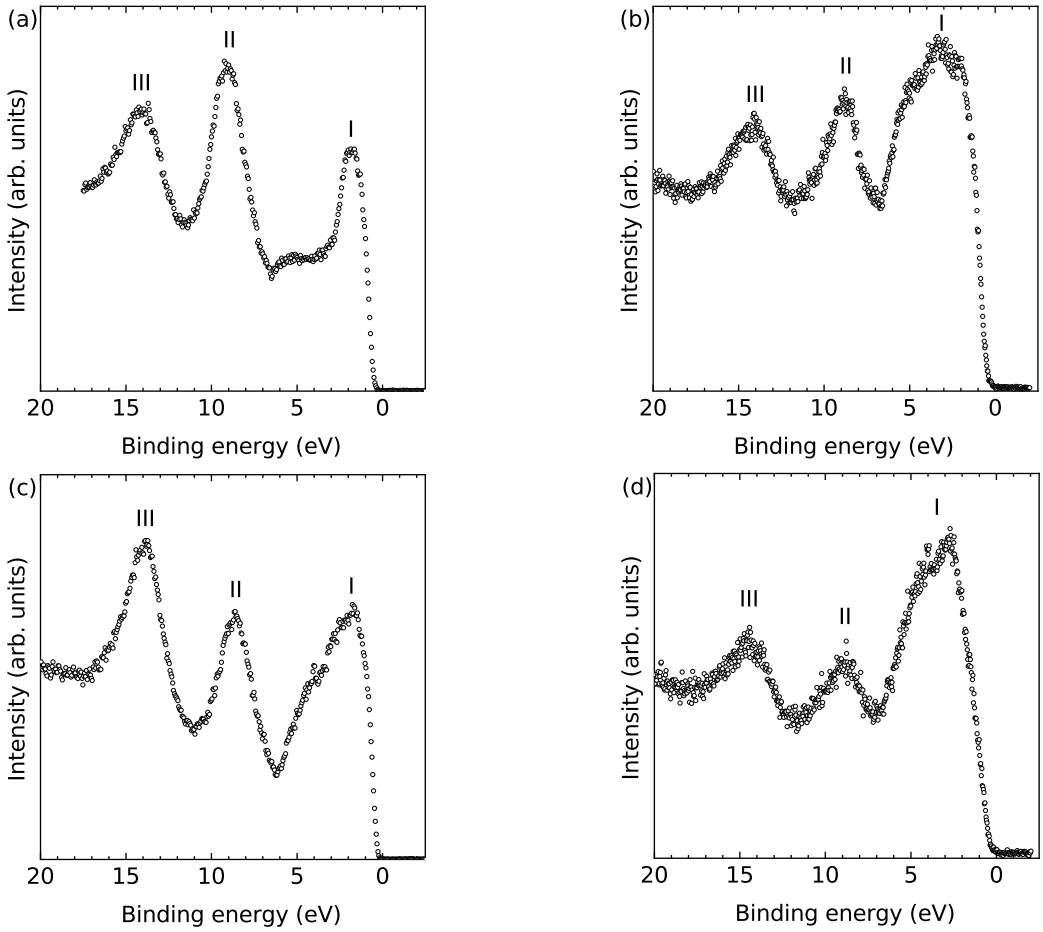

Figure S1: (a) and (b) show HAXPES and XPS measurements of GeS, respectively, while (c) and (d) show HAXPES and XPS measurements of GeSe. Peaks I, II and III are labelled to correspond to how they are referred to in early reports on the valence bands of GeS and GeSe. Peak I was initially thought to be composed of S $3p$/Se $4p$ and Ge $4p$ orbitals, Peak II of Ge $4s$ orbitals, and Peak III of S $3s$/Se $4s$ states.

X-ray diffraction

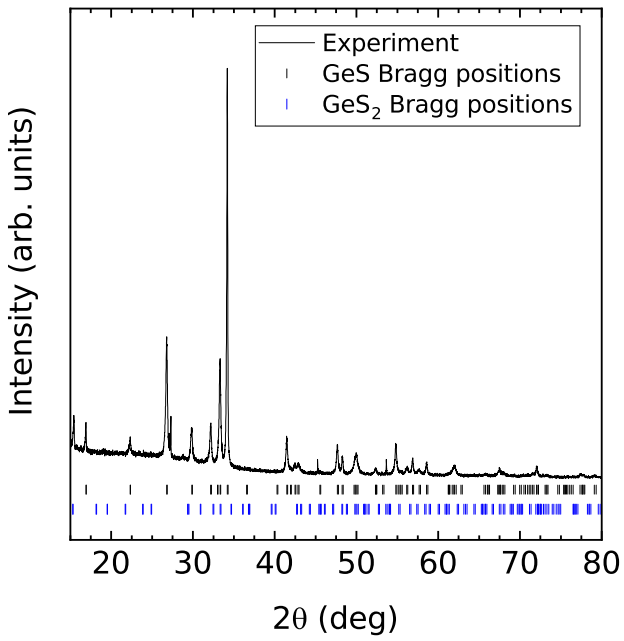

Figure S2: Cu K_α x-ray diffraction pattern collected from GeS crystals ground into powder. The data shows that the powder is predominantly GeS with no trace of GeS_2 (the most intense peak for GeS_2 is expected at 18°). The Bragg positions for GeS are calculated based on an orthorhombic *Pnma* structure with lattice parameters $a = 10.47883$ Å, $b = 3.64229$ Å, and $c = 4.30520$ Å. Previously reported Bragg positions for GeS_2 are also shown for comparison.[1,2]

Core level measurements

GeS

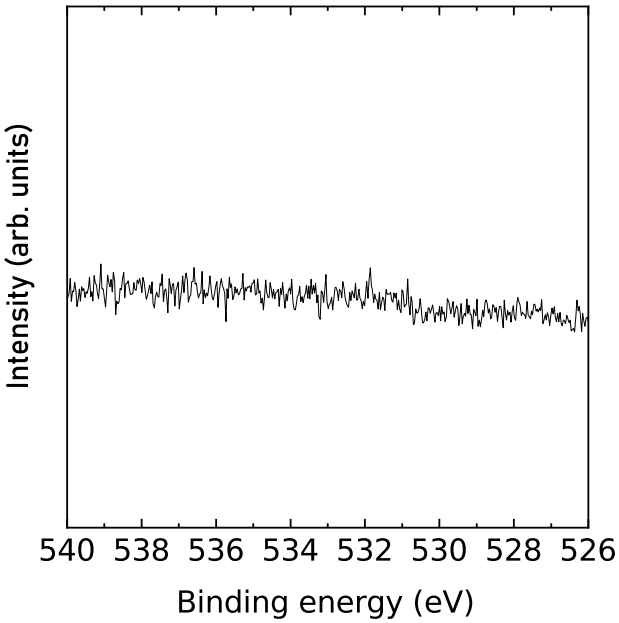

Figure S3: Core-level spectrum of the GeS sample in the O 1s region. A peak near 531 eV is expected if oxygen is present in the sample. This spectrum therefore indicates minimal oxygen contamination at the surface of the sample and accounts for the absence of Ge oxide features in the GeS core level spectra shown in the main manuscript and below.

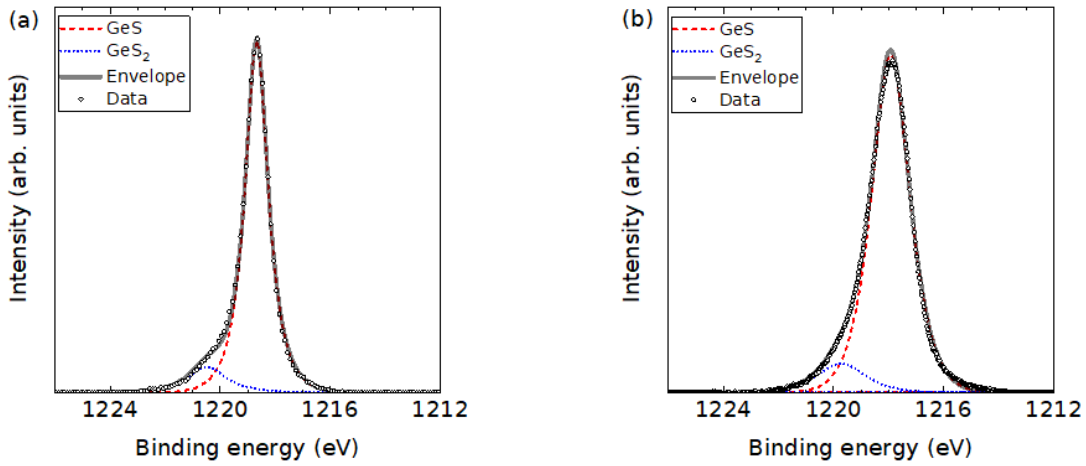

Figure S4: A comparison of (a) HAXPES and (b) XPS measurements and fits of the Ge $2p$ region of the GeS samples. The core level binding energies and FWHM are summarised in Table 1. The separations between peaks are supported by *in situ* XPS measurements (Figure 5), which showed larger amounts of contamination. Both sets of core level spectra have had a Shirley background subtracted.

Table S1: Peak positions (FWHM) (eV) from the fits of the Ge $2p$ core level spectra of GeS shown in Figure S4.

Regions	HAXPES	XPS
Ge $2p_{3/2}$ - GeS	1218.7 (1.0)	1220.5 (1.6)
Ge $2p_{3/2}$ - GeS_2	1220.5 (1.6)	1219.7 (2.1)

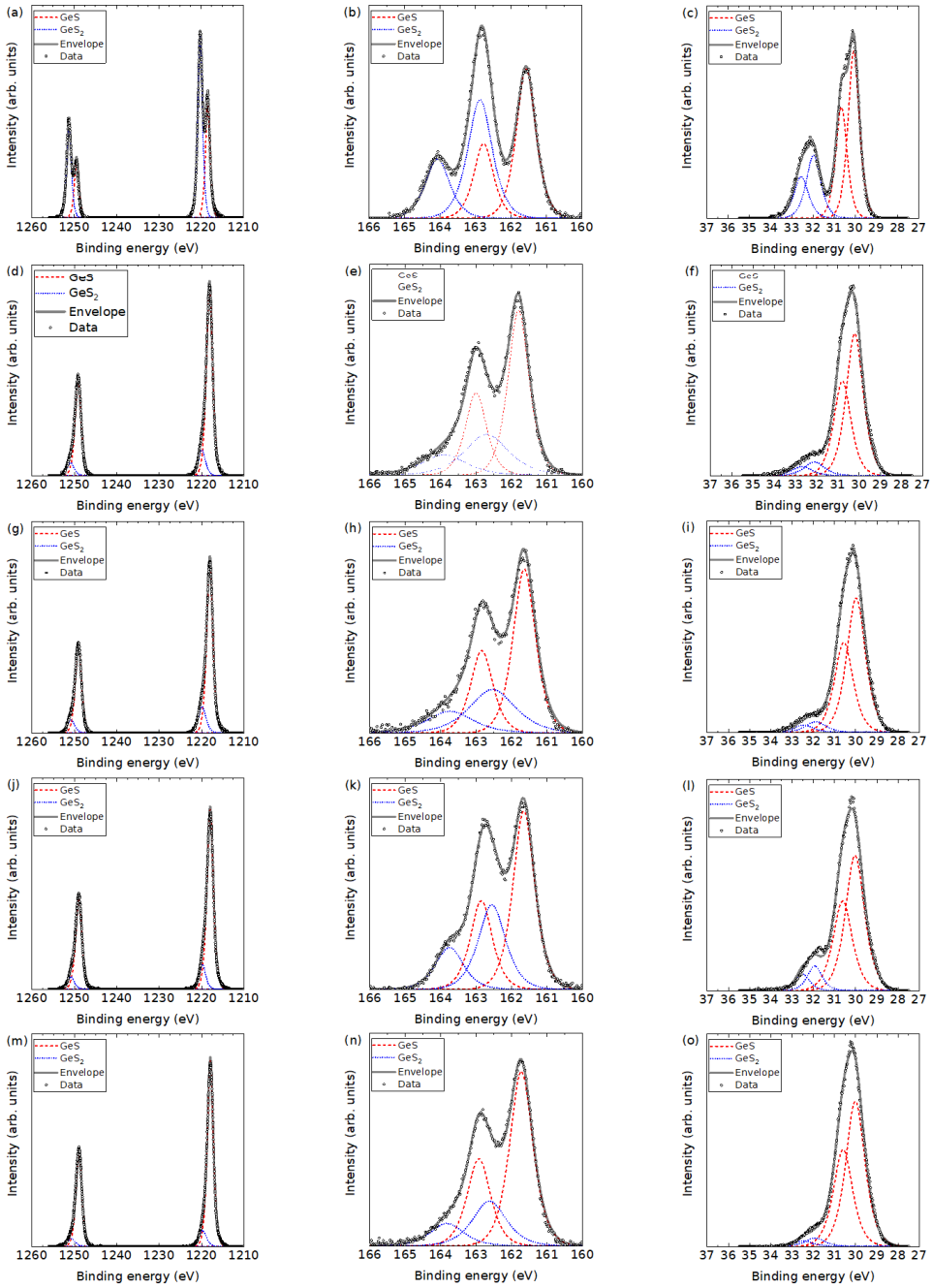

Figure S5: Complete set of XPS measurements performed on the GeS samples in this work. Two separate XPS runs were performed on the same GeS crystal - (a)-(i) without a secondary electron cut-off measurement and (j)-(o) with a secondary electron cut-off measurement. Within these runs core level measurements were taken between sputtering the sample, leading to different levels of contamination. The fits in (n) and (o) are used in Figure 3 in the main manuscript, and part of the fit in (m) is shown in Figure S4. Plots (a), (d), (g), (j) and (m) in the left-hand column show the Ge $2p$ regions, plots (b), (e), (h), (k) and (n) in the central column show the S $2p$ regions, and plots (c), (f), (i), (l) and (o) in the right-hand column show the Ge $3d$ regions. The positions and FWHM of the fitted peaks are summarised in Table 2. All sets of spectra have had a Shirley background subtracted.

Table S2: Peak positions (FWHM) (eV) from the fits of the GeS core level spectra shown in Figure S5. The different runs relate to separate XPS measurements: Runs 1, 2, 3, 4 and 5 relate to Figure 5(a)-(c), Figure 5(d)-(f), Figure 5(g)-(i), Figure 5(j)-(l) and Figure 5(m)-(o), respectively. Runs 1, 2 and 3 are XPS measurements taken without a secondary electron cut off and differ in the time for which the crystal was sputtered *in situ*. Runs 4 and 5 are XPS measurements taken of the same GeS crystal but with a secondary electron cut-off measurement.

Regions	Run 1	Run 2	Run 3	Run 4	Run 5
Ge $2p_{3/2}$ - GeS	1218.3 (1.3)	1218.1 (1.7)	1218.0 (1.7)	1218.0 (1.7)	1217.9 (1.6)
Ge $2p_{3/2}$ - GeS_2	1220.5 (1.6)	1219.9 (1.9)	1219.8 (2.0)	1219.7 (1.7)	1219.7 (2.1)
S $2p_{3/2}$ - GeS	161.6 (0.6)	161.8 (0.6)	161.6 (0.7)	161.7 (0.7)	161.7 (0.8)
S $2p_{3/2}$ - GeS_2	162.9 (0.8)	162.7 (1.5)	162.5 (1.5)	162.6 (0.9)	162.6 (1.1)
Ge $3d_{5/2}$ - GeS	30.0 (0.6)	30.2 (0.9)	30.0 (1.0)	30.0 (1.0)	30.0 (1.1)
Ge $3d_{5/2}$ - GeS_2	31.9 (0.8)	32.1 (1.1)	31.9 (1.1)	31.9 (1.1)	31.9 (1.1)

GeSe

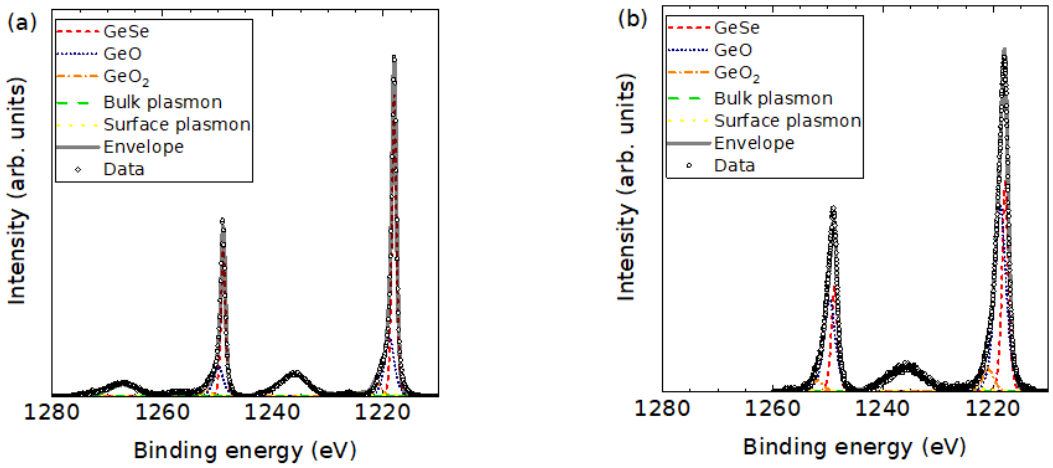

Figure S6: A comparison of (a) HAXPES and (b) XPS measurements and fits of the Ge $2p$ region of the GeSe samples. The core level binding energies and FWHM are summarised in Table S3. The separations between peaks are supported by *in situ* XPS measurements (Figure S7), which showed larger amounts of contamination. Both sets of spectra have had a Shirley background subtracted.

Table S3: Peak positions (FWHM) (eV) from the fits of the Ge $2p$ core level spectra of GeSe shown in Figure 6.

Regions	HAXPES	XPS
Ge $2p_{3/2}$ - GeSe	1218.0 (0.9)	1217.8 (1.3)
Ge $2p_{3/2}$ - GeO	1218.8 (2.0)	1218.7 (2.3)
Ge $2p_{3/2}$ - GeO_2	1221.1 (1.7)	1220.9 (2.2)
Ge $2p_{3/2}$ - Bulk plasmon loss	1236.2 (5.9)	1236.0 (7.3)
Ge $2p_{3/2}$ - Surface plasmon loss	1223.4 (8.0)	1223.2 (4.8)

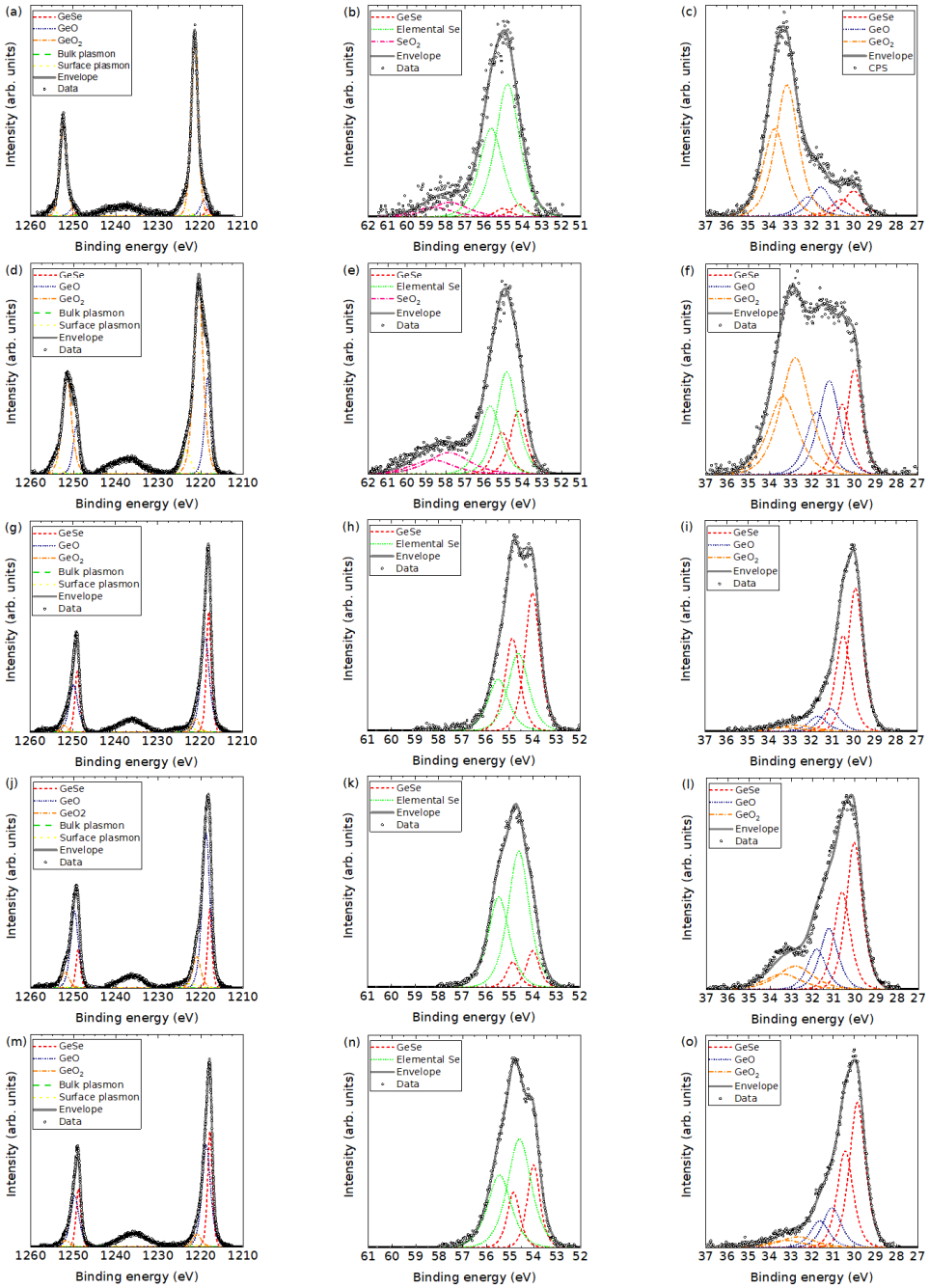

Figure S7: Complete set of XPS measurements performed on the GeSe samples in this work. Two separate XPS runs were performed on the same GeSe crystal - (a)-(i) without a secondary electron cut-off measurement and (j)-(o) with a secondary electron cut-off measurement. Within these runs core level measurements were taken between sputtering the sample, leading to different levels of contamination. The fits in (n) and (o) are used in Figure 4 in the main manuscript, and part of the fit in (m) is shown in Figure 6. Plots (a), (d), (g), (j) and (m) show the Ge $2p$ regions, plots (b), (e), (h), (k) and (n) show the Se $3d$ regions, and plots (c), (f), (i), (l) and (o) show the Ge $3d$ regions. The positions and FWHM of the fitted peaks are summarised in Table 4. All sets of spectra have had a Shirley background subtracted.

Table S4: Peak positions (FWHM) (eV) of the GeSe core level spectra shown in Figure 7. The different runs relate to separate XPS measurements. Runs 1, 2, 3, 4 and 5 relate to Figure 7(a)-(c), Figure 7(d)-(f), Figure 7(g)-(i), Figure 7(j)-(l) and Figure 7(m)-(o), respectively. Run 1, 2 and 3 are XPS measurements taken without a secondary electron cut off measurement and differ in the time for which the crystal was sputtered *in situ*. Runs 4 and 5 are XPS measurements taken of the same GeSe crystal but with a secondary electron cut-off measurement.

Regions	Run 1	Run 2	Run 3	Run 4	Run 5
Ge $2p_{3/2}$ - GeSe	1218.3 (1.3)	1217.5 (1.4)	1217.9 (1.3)	1217.9 (1.1)	1217.8 (1.3)
Ge $2p_{3/2}$ - GeO	1219.1 (2.0)	1218.3 (1.8)	1218.8 (2.4)	1218.7 (2.1)	1218.7 (2.3)
Ge $2p_{3/2}$ - GeO_2	1221.3 (1.8)	1220.5 (2.5)	1221.0 (1.7)	1220.9 (2.2)	1220.9 (2.2)
Ge $2p_{3/2}$ - Bulk pl.	1238.2 (9.3)	1237.4 (7.7)	1236.1 (6.3)	1236.1 (5.9)	1236.0 (7.3)
Ge $2p_{3/2}$ - Surface pl.	1224.2 (2.4)	1223.4 (2.3)	1223.3 (5.5)	1223.3 (5.4)	1223.2 (4.8)
Se $3d_{5/2}$ - GeSe	54.2 (0.9)	54.2 (0.9)	54.0 (0.7)	54.0 (0.6)	54.0 (0.6)
Se $3d_{5/2}$ - El. Se	54.8 (1.5)	54.8 (1.3)	54.6 (1.0)	54.6 (1.1)	54.6 (1.2)
Se $3d_{5/2}$ - SeO_2	57.8 (2.2)	57.8 (2.5)	-	-	-
Ge $3d_{5/2}$ - GeSe	30.0 (1.1)	30.0 (0.8)	29.9 (0.8)	30.0 (0.9)	29.8 (0.9)
Ge $3d_{5/2}$ - GeO	31.6 (1.1)	31.2 (1.2)	31.1 (1.0)	31.2 (1.0)	31.1 (1.0)
Ge $3d_{5/2}$ - GeO_2	33.2 (1.3)	32.8 (1.6)	32.7 (1.9)	32.8 (2.0)	32.7 (1.9)

Density of states

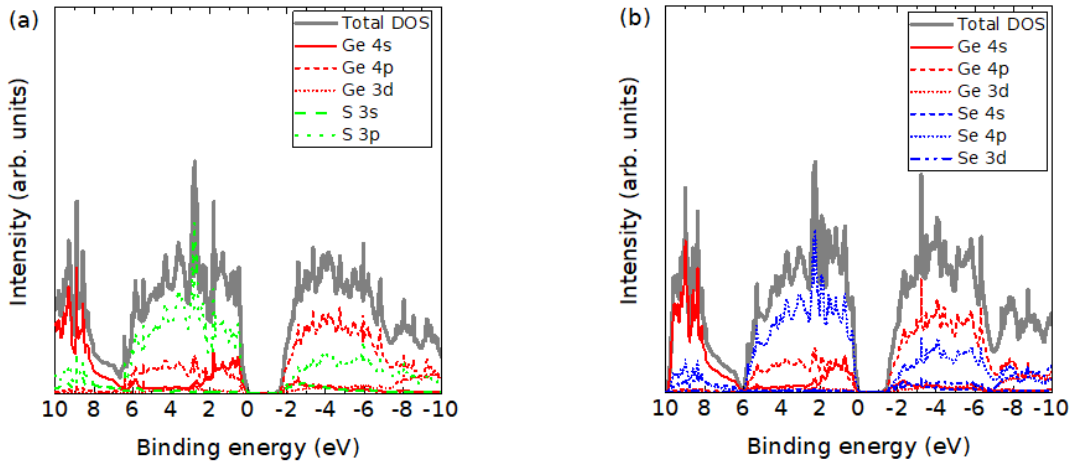

Figure S8: Atom- and orbital-projected electronic density of states (PDoS) of (a) GeS and (b) GeSe, without broadening or cross-section correction.

Ge pseudopotential comparison

Table S5: Calculated lattice parameters of GeS and GeSe obtained using PBEsol+D3 from calculations with pesudopotentials including the Ge $3d$ electrons in the valence region ("Ge $3d$") and treating them as core states ("Ge").

	GeS		GeSe	
	Ge $3d$	Ge	Ge $3d$	Ge
a [Å]	4.150	4.136	4.352	4.328
b [Å]	10.229	10.241	10.783	10.798
c [Å]	3.643	3.656	3.848	3.863
V [Å^3]	154.63	154.86	180.55	180.55

Table S6: Calculated direct and indirect bandgaps ($E_{\mathrm{g,dir}}/E_{\mathrm{g,indir}}$) of GeS and GeSe obtained at the HSE 06 level of theory from calculations using pesudopotentials including the Ge $3d$ electrons in the valence region ("Ge $3d$") and treating them as core states ("Ge").

	GeS		GeSe	
	Ge $3d$	Ge	Ge $3d$	Ge
$E_{\mathrm{g,dir}}$ [eV]	1.678	1.685	1.350	1.339
$E_{\mathrm{g,indir}}$ [eV]	1.349	1.351	1.191	1.158

Table S7: Calculated atomic charges q_{at} and volumes V_{at} of the eight atoms in the GeS unit cell obtained from topological analysis of the HSE 06 charge density.[3] Two sets of values are given: one obtained using pesudopotentials including the Ge $3d$ electrons in the valence region ("Ge $3d$"), and the second from potentials treating them as core states ("Ge").

	q_{at} [e]		V_{at} [Å^3]	
	Ge $3d$	Ge	Ge $3d$	Ge
Ge(1)	0.90	0.88	16.38	16.42
Ge(2)	0.90	0.88	16.38	16.42
Ge(3)	0.90	0.88	16.38	16.42
Ge(4)	0.90	0.88	16.38	16.42
S(1)	-0.90	-0.88	22.28	22.30
S(2)	-0.90	-0.88	22.28	22.30
S(3)	-0.90	-0.88	22.28	22.30
S(4)	-0.90	-0.88	22.28	22.30

Table S8: Calculated atomic charges q_{at} and volumes V_{at} of the eight atoms in the GeSe unit cell obtained from topological analysis of the HSE 06 charge density.[3] Two sets of values are given: one obtained using pesudopotentials including the Ge $3d$ electrons in the valence region ("Ge $3d$"), and the second from potentials treating them as core states ("Ge").

	q_{at} $[e]$		V_{at} [Å^3]	
	Ge $3d$	Ge	Ge $3d$	Ge
Ge(1)	0.74	0.71	18.69	18.72
Ge(2)	0.74	0.71	18.69	18.72
Ge(3)	0.74	0.71	18.69	18.72
Ge(4)	0.74	0.71	18.69	18.72
Se(1)	-0.74	-0.71	26.45	26.41
Se(2)	-0.74	-0.71	26.45	26.41
Se(3)	-0.74	-0.71	26.45	26.41
Se(4)	-0.74	-0.71	26.45	26.41

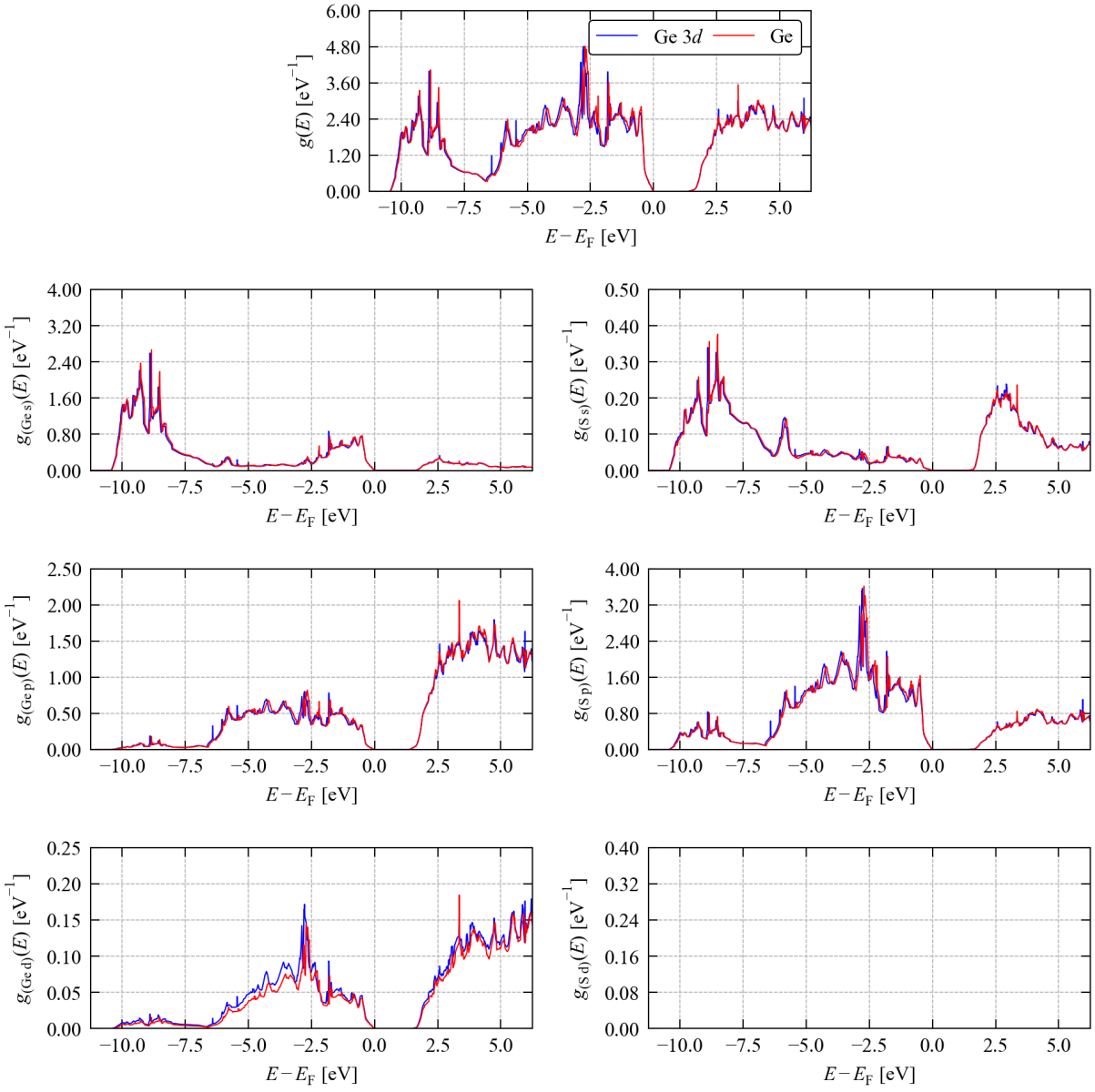

Figure S9: Calculated atom- and orbital-projected electronic density of states (pDoS) of GeS obtained at the HSE 06 level of theory from calculations using pesudopotentials including the Ge $3d$ electrons in the valence region ("Ge $3d$", blue) and treating them as core states ("Ge", red).

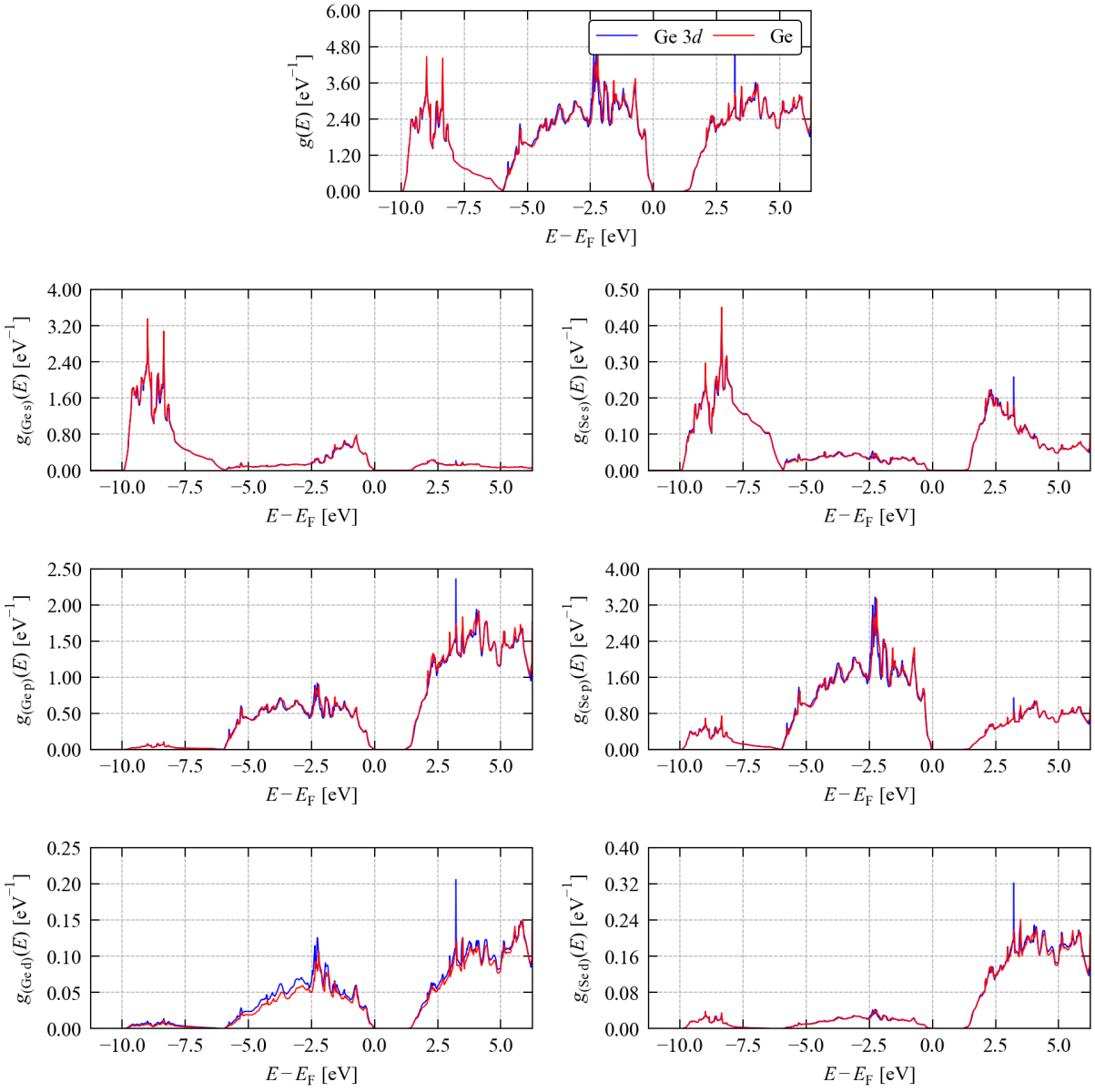

Figure S10: Calculated atom- and orbital-projected electronic density of states (pDoS) of GeSe obtained at the HSE 06 level of theory using pesudopotentials including the Ge $3d$ electrons in the valence region ("Ge $3d$", blue) and treating them as core states ("Ge", red).

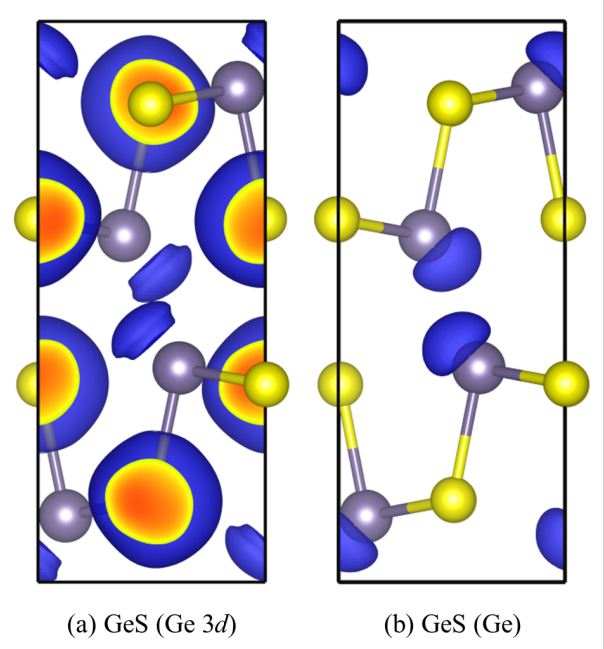

Figure S11: Electron localisation functions[4] of GeS calculated at the HSE 06 level of theory using pesudopotentials including the Ge $3d$ electrons in the valence region (a; "Ge $3d$") and treating them as core states (b; "Ge"). Isosurface levels: (a) 0.65, (b) 0.925. These images were prepared using VESTA.[5]

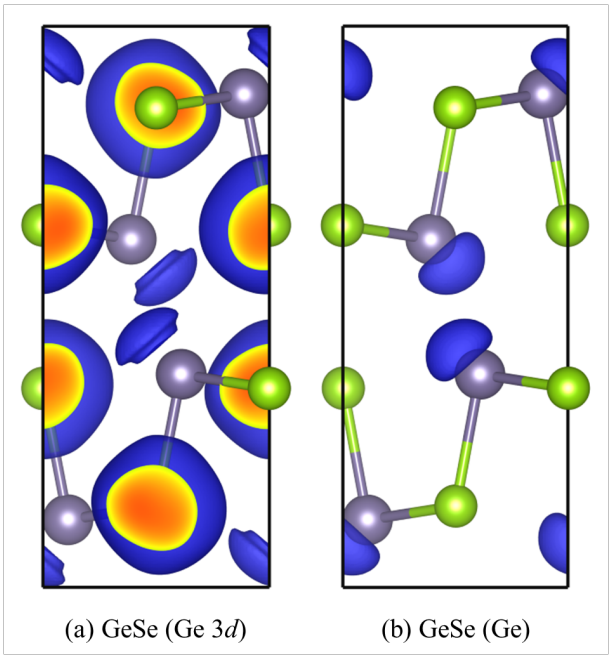

Figure S12: Electron localisation functions[4] of GeSe calculated at the HSE 06 level of theory using pesudopotentials including the Ge $3d$ electrons in the valence region (a; "Ge $3d$") and treating them as core states (b; "Ge"). Isosurface levels: (a) 0.65, (b) 0.925. These images were prepared using VESTA.[5]

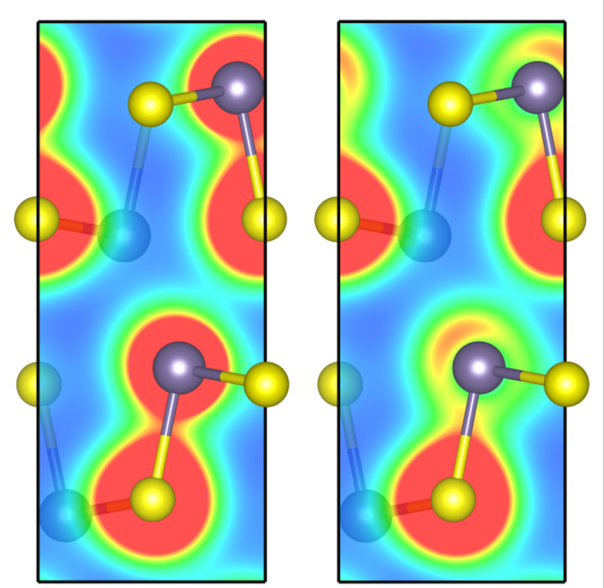

Figure S13: Charge density of GeS calculated at the HSE 06 level of theory using pesudopotentials including the Ge $3d$ electrons in the valence region (a; "Ge $3d$") and treating them as core states (b; "Ge"). Each image shows a cut through the ab plane at a distance of $0.75c$ from the origin, which bisects two of the Ge atoms. The cut shows contour values in the range of [0, 0.5] e Å^{-3}. These images were prepared using VESTA.[5]

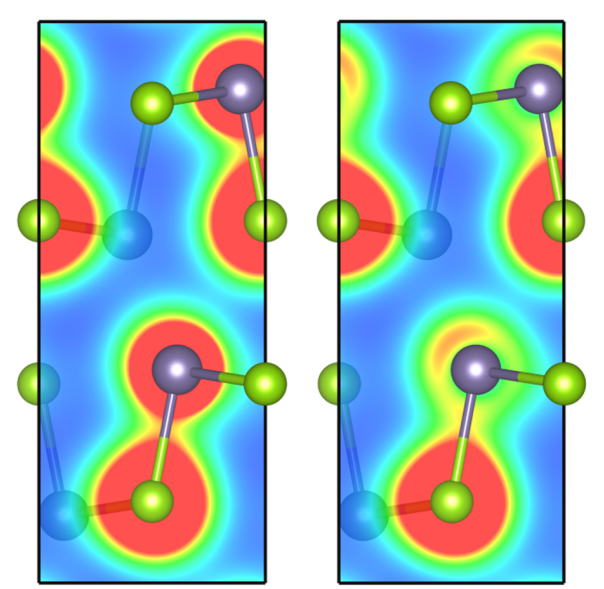

(a) GeSe (Ge 3*d*) (b) GeSe (Ge)

Figure S14: Charge density of GeSe calculated at the HSE 06 level of theory using pesudopotentials including the Ge 3*d* states in the valence region (a; "Ge 3*d*") and treating them as core states (b; "Ge"). Each image shows a cut through the *ab* plane at a distance of 0.75*c* from the origin, which bisects two of the Ge atoms. The cut shows contour values in the range of [0, 0.5] e Å^{-3}. These images were prepared using VESTA.[5]

Effects of compression and expansion

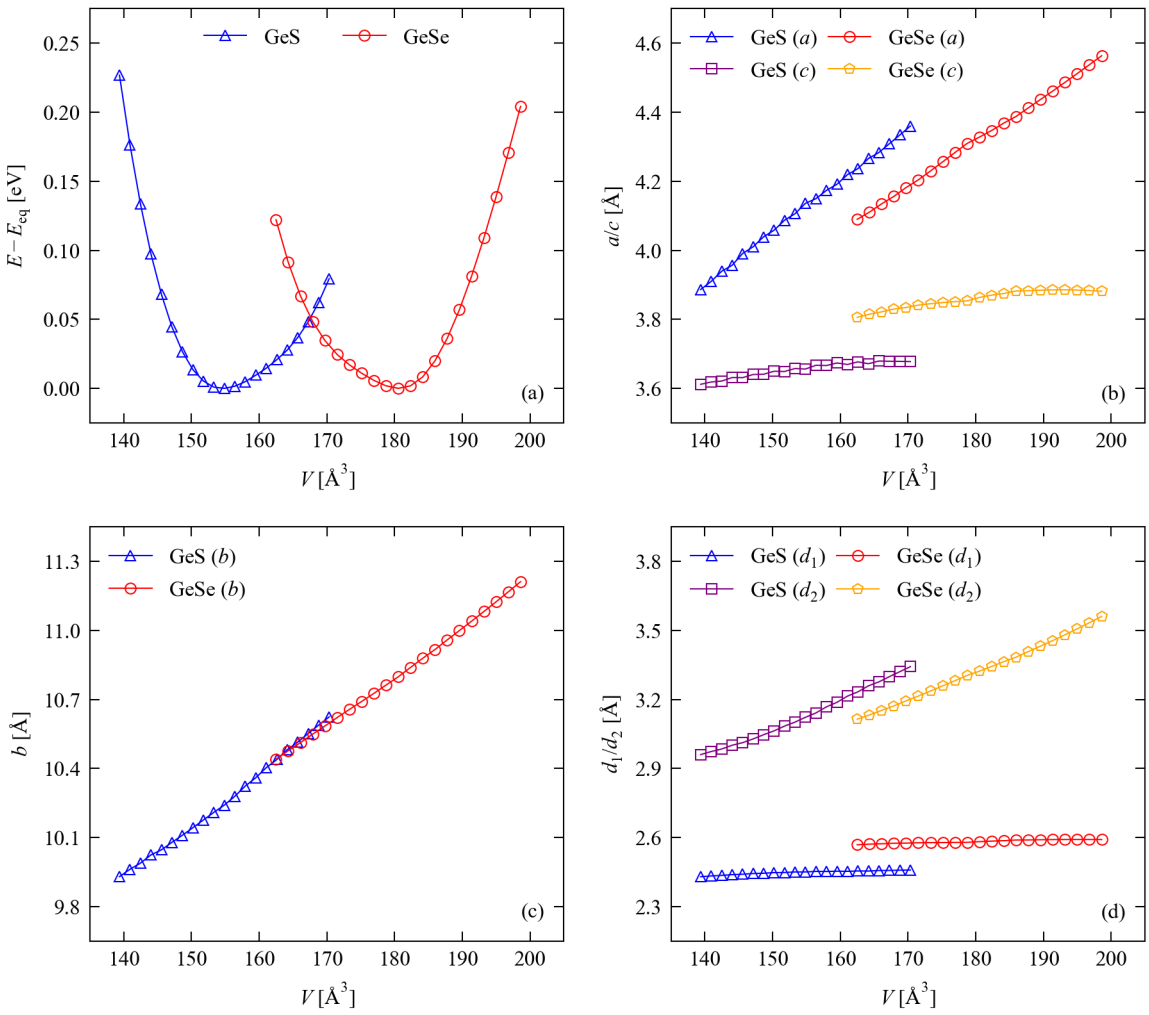

Figure S15: Change in the structure of GeS and GeSe as the unit-cell volume is adjusted between ± 10 % of the calculated equilibrium V_{eq}: (a) energy change $E - E_{eq}$; (b) a/c axis lengths; (c) b axis length; (d) first- and second neighbour Ge-chalcogen distances d_1/d_2. Note that in the calculation models the b axis corresponds to the layering direction. These calculations were performed using pesudopotentials treating the Ge $3d$ electrons as core states.

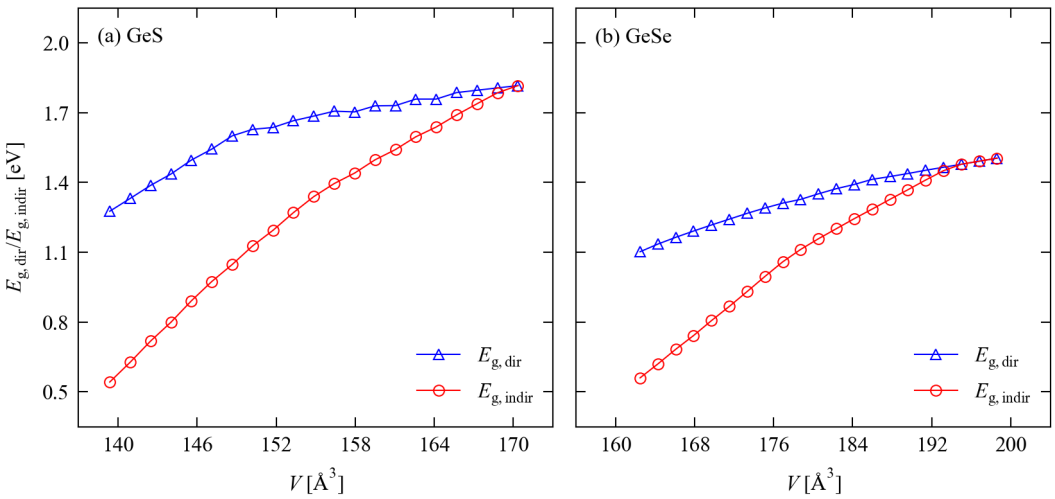

Figure S16: Change in the direct and indirect bandgaps $E_{\mathrm{g,dir}}/E_{\mathrm{g,indir}}$ (blue triangles/red circles) of GeS (a) and GeSe (b) as the unit-cell volume is adjusted between $\pm$ 10 % of the calculated equilibrium volume V_{eq}. The electronic-structure calculations were performed at the HSE06 level of theory and using pesudopotentials treating the Ge $3d$ electrons as core states.

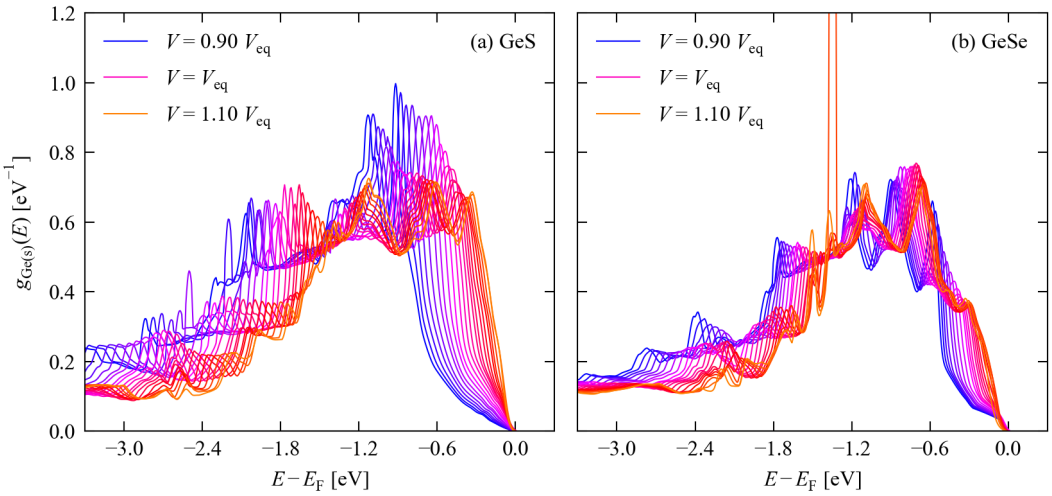

Figure S17: Change in the Ge s projected density of states (DoS) in GeS (a) and GeSe(b) in the vicinity of the valence-band maximum as the unit-cell volume is adjusted between ± 10 % of the calculated equilibrium volume V_{eq}. The lines are colour coded by cell volume from blue (10 % compression) to orange (10 % expansion). The DoS curves have been smoothed by convolution with a narrow Gaussian function ($\sigma = 0.025$ eV) to allow for easier comparison. The sharp feature in the DoS curve for GeSe with $V = 1.09\ V_{eq}$ is an artefact of the tetrahedron method used to integrate the electronic Brillouin zone. The DoS calculations were performed at the HSE06 level of theory and using pesudopotentials treating the Ge $3d$ electrons as core states.

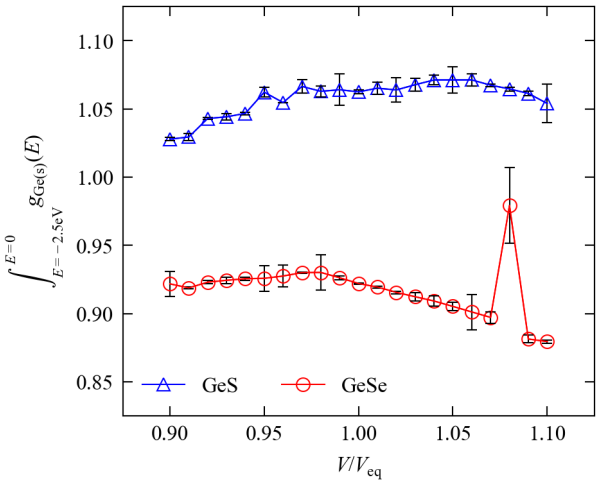

Figure S18: Numerical integral of the Ge s projected density of states (DoS) in Fig. S17 from $E - E_F$ = -2.5 → 0 eV. The error bars show ± the estimated error in the integrals. As noted above, the "spike" for GeSe at $V = 1.09\ V_{eq}$ is due to an artefact in the corresponding DoS function.

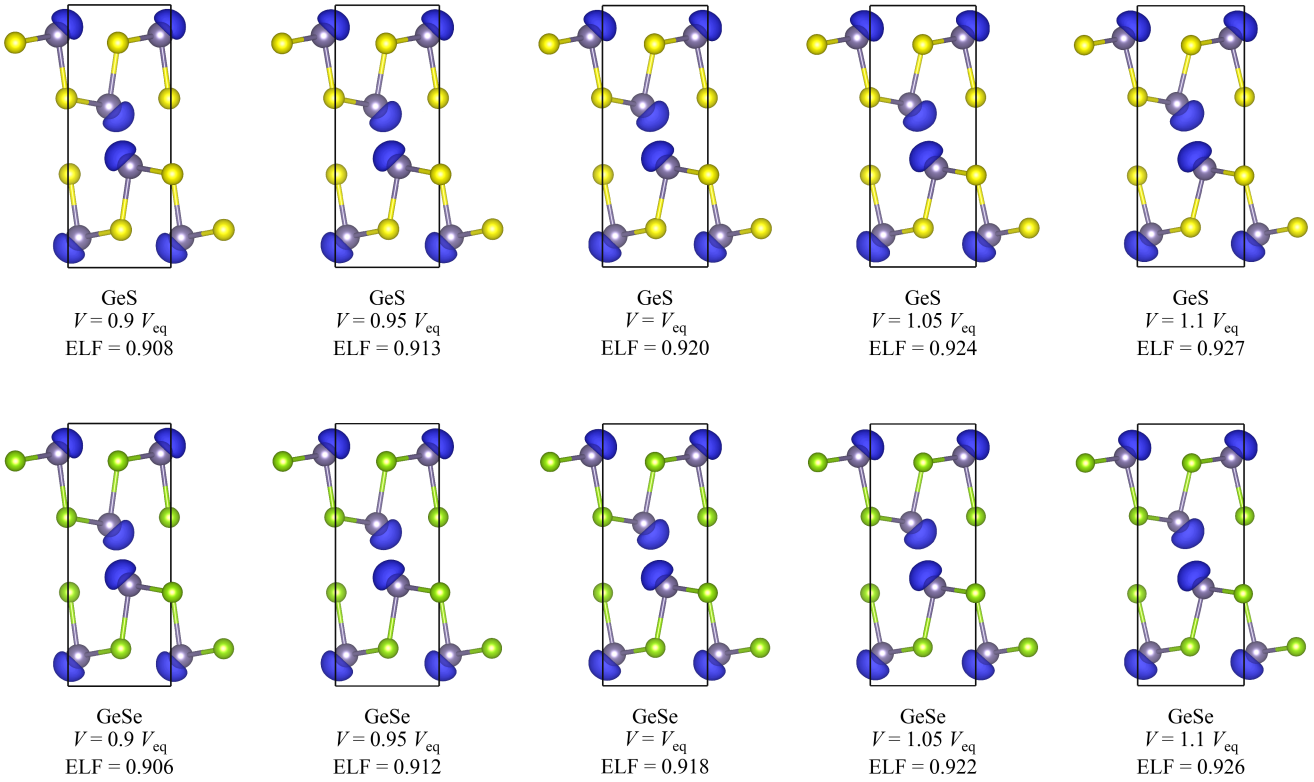

Figure S19: Calculated electron-localisation functions (ELFs) of GeS and GeSe at volumes between ± 10 % of the equilibrium volume V_{eq}. The ELF isosurface values have been adjusted to show the Ge lone pairs at similar spatial extents. These calculations were performed at the HSE06 level of theory and using pesudopotentials treating the Ge $3d$ electrons as core states. The images were prepared using VESTA.[5]

References

(1) Zachariasen, W. H. The Crystal Lattice of Germano Sulphide, GeS. *Phys. Rev.* **1932**, *40*, 917–922.

(2) Zachariasen, W. H. The Crystal Structure of Germanium Disulphide. *The Journal of Chemical Physics* **1936**, *4*, 618–619.

(3) Henkelman, G.; Arnaldsson, A.; Jónsson, H. A fast and robust algorithm for Bader decomposition of charge density. *Computational Materials Science* **2006**, *36*, 354–360.

(4) Silvi, B.; Savin, A. Classification of chemical bonds based on topological analysis of electron localization functions. *Nature* **1994**, *371*, 683–686.

(5) Momma, K.; Izumi, F. VESTA 3 for three-dimensional visualization of crystal, volumetric and morphology data. *J. Appl. Crystallogr.* **2011**, *44*, 1272–1276.